Methanol Chemisorption and Reaction on the (111) Crystallographic Plane of NiAl

Sanjay Chaturvedi[†] and Daniel R. Strongin*[,‡]

Chemistry Department, Brookhaven National Laboratory, Upton, New York 11973, and Department of Chemistry, Temple University, Philadelphia, Pennsylvania 19122

Received: November 14, 1997; In Final Form: February 13, 1998

Thermal chemistry of CH_3OH on the (111) crystallographic plane of NiAl has been investigated with temperature-programmed desorption (TPD), synchrotron-based photoelectron spectroscopy, high-resolution electron energy loss spectroscopy (EELS), and X-ray photoelectron spectroscopy (XPS). It is inferred from EELS results that CH_3OH, at least in part, adsorbs molecularly at 120 K and completely converts to methoxy, $CH_3O_{(ad)}$, by 200 K. Photoelectron spectroscopy indicates that the majority of methoxy binds strongly to the Al component, inducing a 1 eV shift of the Al 2p core level to higher binding energy, relative to the same Al core level of clean NiAl(111). Comparison of EELS results for methoxy on NiAl(110) and NiAl(100) to NiAl(111) opens up the possibility that methoxy adopts at least two different binding sites on the (111) plane of NiAl. One of these sites has a strong contribution from Ni, and a second site has a lesser contribution from Ni (i.e., "Al-rich" site), and methoxy decomposition on this latter site leads to no oxygenated gaseous product. Thermal decomposition of methoxy results in the production of gaseous H_2, CO, CH_4, and CH_3 in the temperature range 200−650 K (aluminum oxide forms by 650 K). It is thought that CO and probably CH_4 result from the decomposition of methoxy on the "Al site" with strong Ni character.

1. Introduction

Surface reactions occurring on alloys are strongly affected by the geometric structure and atomic composition of the near surface region.[1] Development of an understanding of the structure−reactivity relationship for alloys is often difficult due to significant uncertainties in the surface structure. Research presented in this contribution investigates the surface reactivity of the NiAl alloy. While there remain outstanding surface structural issues concerned with NiAl, this alloy does provide a bimetallic system that exhibits good long-range order and low Miller indice planes that have a rather well-defined surface composition and structure. Prior research in our laboratory has used methanol as a probe molecule to address the surface reactivity of the (110) and (100) planes of NiAl. Research presented in this contribution examines this same adsorbate on the (111) crystallographic plane of NiAl and completes our study of the three low Miller indice planes of NiAl.

Methanol serves as a revealing probe molecule on the NiAl alloy, since the chemistry of this adsorbate is markedly different on Ni and Al surfaces. Also, in general the interactions of alcohols with well-defined solid surfaces have been a subject of both fundamental and practical interest due to the industrial importance of the surface-catalyzed methanol synthesis reaction.[2−5] Furthermore, the surface reactivity of NiAl may have particular relevance to understanding the mechanism of this reaction, since it has been suggested that under catalytic conditions Ni−Al intermetallic and Ni−Al−O phases may exist on the Ni/Al_2O_3 catalyst.[6]

CH_3OH is known to undergo O−H bond cleavage on both Al[7−10] and Ni[11−20] single crystals to form surface methoxy, CH_3O. On Al, this species undergoes C−O bond cleavage near 450 K to form gaseous CH_4.[7−10] In contrast, there is no thermally induced C−O bond cleavage within the methoxy intermediate on Ni, but rather this species undergoes dehydrogenation reactions near 260 K to form CO that desorbs later at 400 K.[12−17] Prior studies of methanol on NiAl(110) and NiAl(100) have shown that methoxy decomposition on the former surface results in a greater yield of CO and methane production.[21] This difference has been attributed to the presence of Ni atoms in the outermost layer of NiAl(110)[22,23] [(NiAl(100) is Al terminated[24]] that facilitate hydrogenation reactions. NiAl(111), which is addressed in the present study, is thought to be comprised of Ni and Al individually terminated by 1×1 domains, separated by monatomic steps.[25,26] This surface is quite open compared to the other two surfaces, and surface reactions are expected to be influenced by the direct interaction of the second- and third-layer atoms. Recent research in our laboratory has shown that NiAl(111) shows unique reactivity toward iodomethane and iodoethane relative to the (110) and (100) planes of NiAl.[27a,b]

In this study, we investigate the reactions of CH_3OH on NiAl(111) in the ultrahigh-vacuum (UHV) environment and compare selected results to those obtained previously for NiAl(110) and NiAl(100) surfaces. Synchrotron-based photoelectron spectroscopy results presented in this contribution suggest that CH_3OH adsorbs on NiAl(111) at 120 K primarily in an associative manner. High-resolution electron energy loss spectroscopy (EELS) results indicate that CH_3OH undergoes facile O−H bond cleavage on NiAl(111) [similarly on NiAl(110) and NiAl(100)] to form methoxy ($-OCH_3$) at temperatures as low as 150 K. Photoelectron spectroscopy shows that the majority of methoxy binds strongly to the Al component of NiAl in the outermost layer. EELS suggests that methoxy adopts at least two types of binding sites on NiAl(111): a site strongly influenced by Ni and another that is "Al-like". Facile decom-

* To whom correspondence should be addressed. Tel (215)204-7119; FAX (215)204-1532; e-mail dstrongi@nimbus.ocis.temple.edu.
[†] Brookhaven National Laboratory.
[‡] Temple University.

S1089-5647(98)00216-8 CCC: $15.00
Published on Web 03/26/1998

position of methoxy occurs as the surface is heated beyond 300 K and yields gaseous products that include H_2, CO, CH_4, and CH_3 radicals. CO product and probably CH_4 result from methoxy decomposition on the Al−Ni site. This inference is generally consistent with prior research that has shown that CO is produced during $CH_3O_{(ad)}$ decomposition on Ni[11−16,19−20,28−30] and Ni/Al_2O_3[31] but not on Al surfaces.[8,9]

2. Experimental Section

All the experiments presented were performed in a bakeable ultrahigh-vacuum (UHV) chamber with a base pressure of 2×10^{-10} Torr. The details of the chamber have been described elsewhere.[27a,32a,b] Briefly, analytical equipment housed in the experimental apparatus consisted of a quadrupole mass spectrometer (QMS), low-energy electron diffraction (LEED) optics, double-pass cylindrical mirror analyzer (CMA), and an X-ray source. Also available was an ion gun for sample cleaning.

The NiAl single-crystal ingot used in the study had a bulk composition of 50 atomic % Ni (supplier was General Electric Aircraft Engines). The crystallographic plane was prepared from this ingot by standard metallurgical methods (e.g., spark cut and polished with diamond paste) and was within 1° of the specified orientation. The sample was approximately 8 mm on a each side with a thickness of 2 mm.

Four Ta support wires (0.25 mm diameter) were spot-welded to each side of the sample, and the ends of the wires were spot-welded to Ta tabs that were mechanically attached to a liquid nitrogen cryostat with cooling capability to 120 K. Heating of the samples was accomplished by passing current through the Ta wires. A chromel−alumel (type K) thermocouple was spot-welded to the back of the sample for accurate temperature measurements.

The sample showed substantial carbon and oxygen contamination when introduced into the experimental chamber. Oxygen was removed from the near surface region by repeated 500 eV argon ion sputter (20 min) and 1200 K anneal (5 min) cycles. Trace amounts of carbon left on the surface after these cycles were removed by heating the particular sample at 1000 K in oxygen (2×10^{-7} Torr) for times ranging from 2 to 10 min depending on the amount of carbon. This procedure removed the carbon without introducing oxygen contamination. A sharp (1×1) LEED pattern was observed after this cleaning procedure.

Methanol (CH_3OH, HPLC grade, Fisher Chemical; CD_3OD, 99.8 atom % D, Cambridge Isotope Laboratories; CD_3OH, 99.5% purity; Sigma Chemical Co.) was used after several freeze−thaw−pump cycles. The purity was confirmed by mass spectroscopy. Methanol was admitted into the chamber through a 0.05 cm diameter dosing tube connected to a UHV compatible leak valve. The NiAl(111) sample was always held at 120 K during exposure to methanol. Dosing of the sample was accomplished by backfilling the experimental chamber with methanol. Exposures quoted in this paper in units of langmuirs (1 langmuir = 10^{-6} Torr·s) are not corrected for the sensitivity of the nude ionization gauge used for pressure measurements.

Temperature-programmed desorption (TPD) experiments were performed by heating the sample at a heating rate of 8 ± 1 K/s. Gases desorbing from the surface were analyzed by a multiplexed QMS capable of simultaneously measuring up to nine ions during a single TPD experiment. The mass spectrometer was housed in a gold-plated stainless shield (with cryogenic capabilities) having a 6.0 mm diameter aperture. During TPD experiments the sample was placed within 2−3 mm of this aperture hole, thereby limiting the detection of gases evolving from the support wires. All the yields of products quoted in this paper have been corrected for their sensitivity of the mass spectrometer.

X-ray photoelectron spectroscopy (XPS) data presented in this paper were acquired with unmonochromatized Mg Kα (1253.6 eV) radiation. The pass energy of the CMA was set at 50 eV during the acquisition of both O and C 1s data. The binding energy scale for the XPS was calibrated by aligning the Ni $2p_{3/2}$ of NiAl to 853.3 eV below the fermi level (E_F). XPS data, as a function of temperature, presented in this paper, were obtained by exposing the sample to methanol at 120 K and then heating the sample at a rate of 8 K/s to the desired temperature. XPS data were recorded after rapidly cooling the sample back to 120 K.

EELS spectra were acquired at a specular detection angle ($\theta_i = \theta_f = 60°$). The incident beam energy was 3.5 eV. The resolution and counting of the primary beam varied from 104 to 144 cm^{-1} and from 3×10^2 to 4×10^3 Hz, respectively, after exposure to methanol. There is an uncertainty of ± 20 cm^{-1} in all the reported vibrational frequencies.

Synchrotron data were acquired at the U7b beamline at the National Synchrotron Light Source (NSLS) at Brookhaven National Laboratory. Photoelectrons emitted from the sample were energy analyzed by a VSW hemispherical analyzer (HA 100) mounted 90° relative to the photon beamport. Valence and Al 2p level spectra were recorded by using a pass energy of 10 eV. The photon energy used to obtain the Al 2p data was 140 eV while 100 eV photons were used to acquire the valence band data.

3. Results

This section presents TPD, synchrotron-based photoelectron spectroscopy, EELS, and XPS data for CH_3OH/NiAl(111). TPD results are presented first and address the types of gaseous products that desorb during the thermal decomposition of CH_3OH on NiAl(111). EELS and synchrotron-based photoelectron spectroscopy address the adsorption of CH_3OH and its subsequent thermally induced chemical transformations on NiAl(111). XPS results are presented last, and these data used along with TPD results allow the relative yield of gaseous products to be estimated and compared to prior results obtained in our laboratory for CH_3OH/NiAl(110) and CH_3OH/NiAl(100).

3.1. TPD Studies of CH_3OH/NiAl(111). Figure 1 exhibits TPD traces for the various gaseous species that desorb from NiAl(111) after it has been exposed to 6.0 langmuirs of methanol at 120 K. Note that some of the traces feature a sharp peak at 140 K. This peak is assigned to methanol desorption from a condensed layer that forms upon adsorption at 120 K. H_2 (*m*/*e* 2), CO (*m*/*e* 28), CH_4 (*m*/*e* 16), and CH_3 (*m*/*e* 15) are the main products that desorb as a result of the thermal decomposition of methanol. Data in the figure show that H_2 desorbs from NiAl(111) in discrete and resolvable states. These different desorption features will be discussed later in light of experiments carried out with deuterated methanol. CO, resulting from the thermal decomposition of CH_3OH, desorbs with a peak maximum at 425 K and exhibits a desorption shoulder at 550 K. CH_4 (*m*/*e* 16) product is detected as two features at 350 and 580 K. The majority of the latter desorption feature is thought to be due to methyl radical desorption from NiAl(111). The rationale for this contention is now presented.

Figure 2a shows desorption traces for various C_1 cracking fragments that result after NiAl(111) is exposed to 3.0 langmuirs of CH_3OH at 120 K. Curves denoted as "x", "y", and "z" correspond to desorption traces for CH_4^+ (*m*/*e* 16), CH_3^+ (*m*/*e*

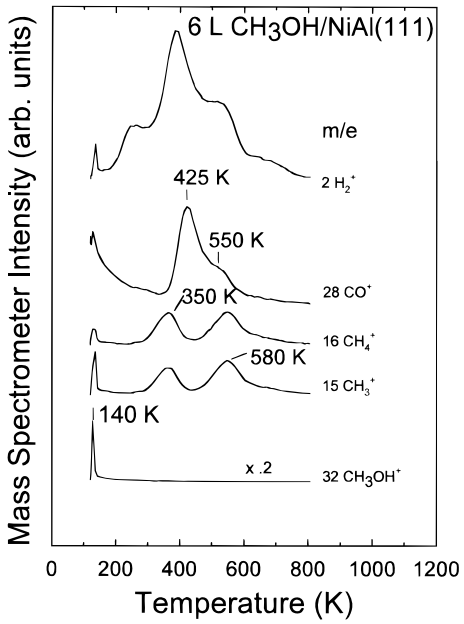

Figure 1. TPD traces of products desorbing from NiAl(111) after a 6.0 langmuir exposure of methanol at 120 K. Gaseous products include H_2 (*m*/*e* 2), CO (*m*/*e* 28), CH_4 (*m*/*e* 16), and CH_3 (*m*/*e* 15).

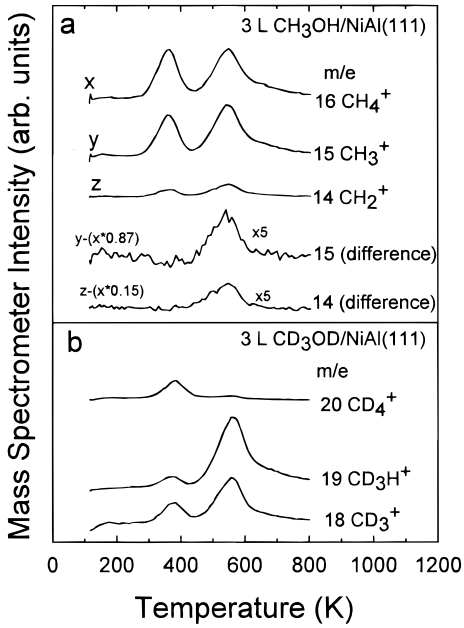

Figure 2. (a) TPD traces of various C_1 products that result from a 3.0 langmuir exposure of CH_3OH/NiAl(111) at 120 K. Curves "x", "y", and "z" correspond to desorption traces for CH_4^+ (*m*/*e* 16), CH_3^+ (*m*/*e* 15), and CH_2^+ (*m*/*e* 14), respectively. The *m*/*e* 15 difference spectrum is obtained by removing the CH_3^+ contribution due to CH_4 cracking from curve "y". The *m*/*e* 14 difference spectrum is obtained by removing the CH_2^+ contribution due to CH_4 cracking from curve "y". (b) TPD traces of CD_4^+ (*m*/*e* 20), CD_3H^+ (*m*/*e* 19), and CD_3^+ (*m*/*e* 18) after NiAl(111) has been exposed to 3 langmuirs of CD_3OD at 120 K.

15), and CH_2^+ (*m*/*e* 14), respectively. The *m*/*e* 15 difference spectrum of the figure is obtained by removing the CH_3^+ contribution due to CH_4 cracking from the raw intensity of CH_3^+ (i.e., curve "y"). For our mass spectrometer settings the *m*/*e* 15:16 ratio for the cracking of CH_4 is 0.87. Hence, the difference spectrum is arrived at by multiplying the *m*/*e* 16 (curve "x") spectrum by 0.87 and then subtracting the result from the *m*/*e* 15 data. The resulting difference spectrum does not show a desorption feature at 350 K. This result suggests that the 350 K desorption feature in the *m*/*e* 15 and 16 spectra is due to CH_4 product that forms on NiAl(111). Further support of this contention is obtained by analyzing the *m*/*e* 14 difference spectrum, obtained by removing the CH_4 cracking contribution from the *m*/*e* 14 spectrum. For our spectrometer settings, the ratio of CH_4:CH_3:CH_2 for CH_4 is 1:0.87:0.15, and hence the *m*/*e* 14 difference spectrum is obtained by first multiplying the *m*/*e* 16 data by a 0.15 factor and then subtracting the result from the *m*/*e* 14 data. As was the case for the *m*/*e* 15 difference spectrum, there is no 350 K desorption feature in the *m*/*e* 14 difference spectrum, suggesting again that this desorption feature is due to CH_4 desorbing from the sample.

Both the *m*/*e* 14 and 15 difference spectra, however, exhibit a desorption feature at 580 K, suggesting that the entire feature at 580 K in the *m*/*e* 14 and 15 spectra cannot be due to the cracking of CH_4 in the mass spectrometer. We believe that at least a fraction of the *m*/*e* 15 intensity at 580 K is due to the desorption of CH_3 radical from NiAl(111). This statement is supported by further analysis of the data that shows that the *m*/*e* 15:14 difference spectrum peak area ratio of the 580 K desorption features is 0.45, close to the literature values (0.42,[33] 0.54[34]) for the cracking pattern of gaseous CH_3.

To investigate the possibility of methyl desorption more closely, Figure 2b presents TPD traces for CD_4^+ (*m*/*e* 20), CD_3H^+ (*m*/*e* 19), and CD_3^+ (*m*/*e* 18) after NiAl(111) is exposed to 3.0 langmuirs of CD_3OD at 120 K. These data show that there is no high-temperature feature at 580 K in the *m*/*e* 20 trace, suggesting that CD_4 is not a reaction product formed on NiAl(111). This experimental observation indicates that the 580 K feature in the *m*/*e* 18 trace is not due to the cracking of CD_4 product. Instead, we believe that this feature in the *m*/*e* 18 trace is due to CD_3 desorption from NiAl(111) and also from the cracking of CD_3H product (*m*/*e* 19 trace). It is speculated that the latter product is formed from the reaction of CD_3 product with the walls of the experimental chamber (i.e., $CD_3 + H_{(ad)} \rightarrow CD_3H$).[35] This inference also leads us to speculate that the 580 K CH_4 feature in Figure 2a is due, at least in part, to the desorption of CH_3 from NiAl(111) during the thermal decomposition of CH_3OH and subsequent reaction with the interior walls of the experimental apparatus. In view of this point, there is the possibility that CH_3 is the sole reaction product that desorbs at 580 K. Methyl radical ejection from both methanol-dosed (110) and (100) surfaces of NiAl occurs at a similar temperature.[21,32a]

Figure 3a exhibits H_2 desorption traces after NiAl(111) is exposed to CH_3OH. Three broad desorption states at ~250, 400, and 550 K grow in with increasing CH_3OH exposure. Some insight into the details of these states is obtained by examining TPD for CD_3OH/NiAl(111) shown in Figure 3b. H_2 desorbs with a peak maximum of (350 K), and the desorption of this species is thought to be limited by its own desorption kinetics and not reaction rate limited by O−H bond cleavage. Spectroscopic data presented later suggest that the O−H bond in CH_3OH is broken by 200 K. In contrast to H_2 desorption, the desorption of D_2 and HD at temperatures higher than 300 K are suspected to be reaction rate limited by C−D bond cleavage.

3.2. EELS of CH_3OH/NiAl(111). Figure 4 displays EELS spectra of NiAl(111) after exposure to 10 langmuirs of CH_3OH at a temperature of 130 K. A 10 langmuir exposure of CH_3OH leads to the formation of a multilayer, and the associated 130 K spectrum in the figure exhibits five EELS features at 750, 1040, 1480, 2950, and 3250 cm^{-1}. On the basis of prior research of solid methanol and condensed methanol on metal surfaces,[1,6,11,15,24] the following assignments are made. The 2950 cm^{-1} mode is assigned to C−H stretching [$\upsilon(CH_3)$], the 3250

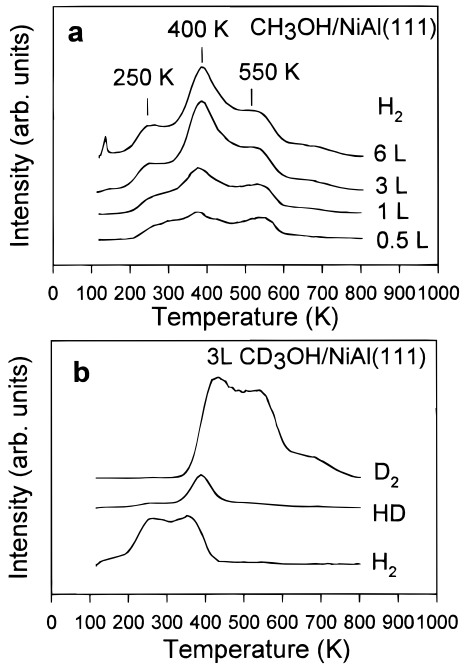

Figure 3. (a) H_2 desorption traces as a function of CH_3OH coverage. (b) TPD traces of D_2, HD, and H_2 after NiAl(111) is exposed to 3.0 langmuirs of CD_3OH at 120 K.

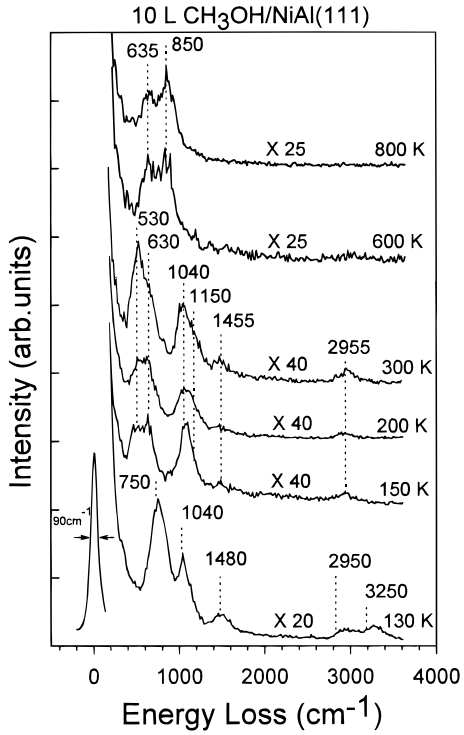

Figure 4. EELS data of a multilayer of CH_3OH adsorbed on NiAl(111) at 120 K and after heating the surface to the indicated temperatures.

cm^{-1} vibration to O−H stretching [υ(OH)], and the 750 cm^{-1} feature to the O−H bending mode [δ(OH)] of CH_3OH. Finally, the EELS features at 1040 and 1480 cm^{-1} are assigned to the C−O stretching [υ(CO)] and CH_3 deformation [$\delta(CH_3)$] modes, respectively. In general, a CH_3 rocking [$\gamma(CH_3)$] mode is observed in the EELS spectrum near 1100 cm^{-1} of solid CH_3OH, and it is suspected that this mode is obscured by the high-energy loss side of the 1040 cm^{-1} mode. Table 1 lists the vibrational frequencies (cm^{-1}) for condensed methanol and $CH_3O_{(ad)}$ on the three surfaces of NiAl. Values for the (110) and (100) surfaces have been obtained from refs 21 and 32a, respectively, and will be used later in the Discussion section.

The majority of the CH_3OH multilayer desorbs by 150 K, and the associated spectrum shows that the loss features assigned to the O−H stretching (3250 cm^{-1}) and bending (750 cm^{-1}) modes are eliminated, but EELS features attributed to C−H stretching, CH_3 deformation, CH_3 rocking, and C−O stretching modes largely remain unchanged in both energy position and intensity. On the basis of these observations, we speculate that methoxy, CH_3O(a), is associated with the 150 K spectrum. It is shown in the next section that there is some molecularly adsorbed CH_3OH that is coadsorbed with the methoxy under these experimental conditions. In addition to the loss of features due to the multilayer desorption, two new features appear in the 150 K spectrum at 530 and 630 cm^{-1}. We assign these features to the metal−O stretching mode [υ(M−O)] of methoxy. Isotope labeling experiments that support this assignment are presented below.

Further heating of the methoxy overlayer to 200 K does not cause any appreciable change in the vibrational spectrum, and heating to 300 K results in an increase in the intensity of the 530 cm^{-1} mode. The reason for this change is not known but suspect it may be due to some methoxy dissociation and/or an orientation change of the methoxy or outermost surface of NiAl(111). The former possibility is least likely, since if the 530 cm^{-1} mode is due to the surface−methoxy stretch (which would be expected to be distinguishable from the surface−atomic oxygen stretch), then it would be expected to decrease upon methoxy dissociation. In either circumstance, however, we postulate that the majority of the overlayer is stable to a temperature of 300 K. Marked changes in the EELS spectrum occur upon heating to 600 K, among the most noticeable changes being the loss of the ν(CO) mode at 1040 cm^{-1} and $\nu(CH_3)$ at 2955 cm^{-1}. This experimental observation indicates that the methoxy decomposes and all hydrocarbon fragments desorb from the surface by 600 K. This result is consistent with the TPD results presented in the prior section and is also supported by the results obtained with both synchrotron-based photoemission spectroscopy and XPS presented in the subsequent sections. The 600 K spectrum exhibits spectral features at 635 and 850 cm^{-1} that become sharper upon heating to 800 K. These modes are thought to be associated with the formation of Al oxide on the surface[36−39] or chemisorbed oxygen, since prior research has shown chemisorbed oxygen on Al(111) to exhibit modes at both 635 and 850 cm^{-1} .[40] Prior work done on the oxidation of NiAl(110) by Jaeger et al.[42] also exhibits a very intense mode at 850 cm^{-1}.[41]

Returning to the assignment of the metal−oxygen stretching mode, data in Figure 5 are presented. Spectra in the figure are associated with $CH_3O_{(ad)}$ and $CD_3O_{(ad)}$ and are prepared by individually heating a multilayer of CH_3OH and CD_3OD to 200 K to form the methoxy overlayer. As expected, the C−D stretching frequency for CD_3O is about 750 cm^{-1} lower than the C−H stretching frequency of CH_3O, and the C−O stretching frequency is largely unaffected. Of note is that the modes at ∼530 and 630 cm^{-1} for $CH_3O_{(ad)}$ also are associated with $CD_3O_{(ad)}$ (except for changes in the relative ratio). This similarity is consistent with these modes being due to the surface−oxygen stretch of $CH_3O_{(ad)}$ and $CD_3O_{(ad)}$.

3.3. Synchrotron-Based Photoelectron Spectroscopy. Figure 6 presents valence band spectra of clean NiAl(111) as a function of CH_3OH exposure. Energy positions of the vertical lines indicated at the top of the figure are associated with the ionization potentials of the valence levels of gaseous CH_3OH.[42]

TABLE 1: Comparison of the Vibrational Frequencies (cm^{-1}) for Condensed Methanol and $CH_3O_{(ad)}$ on NiAl(111), NiAl(110)[21,32A] and NiAl(100)[21]

	CH_3OH			$CH_3O_{(ad)}$		
mode	NiAl(110)	NiAl(100)	NiAl(111)	NiAl(110)	NiAl(100)	NiAl(111)
ν(OH)	3230	3260	3250			
$\nu_{as}(CH_3)$	2935	2985	2950	2935	2985	2955
$\delta(CH_3)$	1450	1475	1480	1450	1485	1455
$\gamma(CH_3)$	1145	1150	1150	1155	1150	1150
ν(CO)	1040	1070	1040	1020	1070	1040
δ(OH)	750	765	750			
ν(M−O)				540	640	530, 630

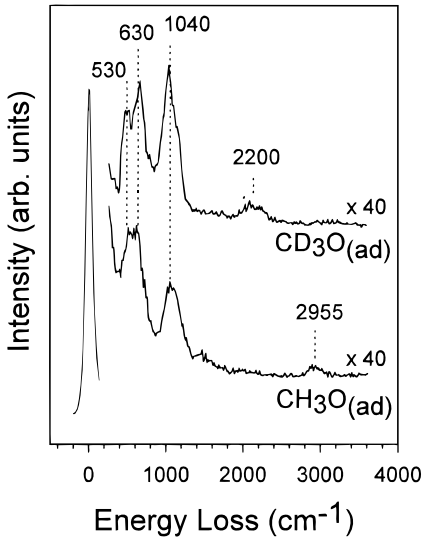

Figure 5. EELS of methoxy species adsorbed on NiAl(111). The surfaces are prepared by individually dosing with CH_3OH and CD_3OD at 120 K and then annealing the surfaces to 200 K to form $CH_3O_{(ad)}$ and $CD_3O_{(ad)}$, respectively. The modes at 530 and 630 cm^{-1} are assigned to surface−OCH_3 stretches and suggest that methoxy binds on at least two distinct sites on NiAl(111).

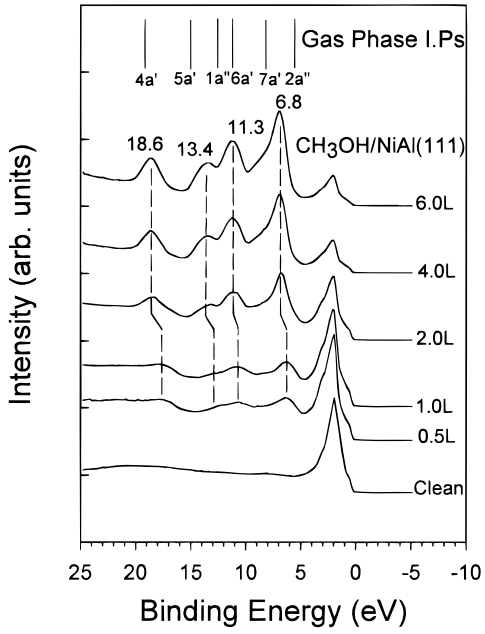

Figure 6. Valence band spectra of NiAl(111) as a function of methanol coverage at 120 K. The vertical lines on top are the ionization potentials of the valence levels of gas-phase CH_3OH.

Gas-phase potentials are measured relative to the vacuum level. To align these levels to the features in our valence band spectrum, which are measured relative to the sample Fermi level, it has been assumed that the more deeply bound 4a′, 5a′ (associated with O−H bond) are least perturbed in the chemisorbed state. Therefore, these two levels of the gas-phase species have been aligned to those corresponding features of the methanol multilayer (6 langmuirs) spectrum (at 18.6 and 13.4 eV, respectively). On the basis of the gas-phase assignments, we then assign the feature at 11.3 to the 1a″ (strong CH_3 character) and 6a′ (which has strong C−O character) levels. The 6.8 eV photoelectron intensity feature is attributed to the 2a″ (localized on the O atom) and 7a′ (H−C−O bonding character and presumed to be a shoulder on the 2a″ feature) level of methanol.

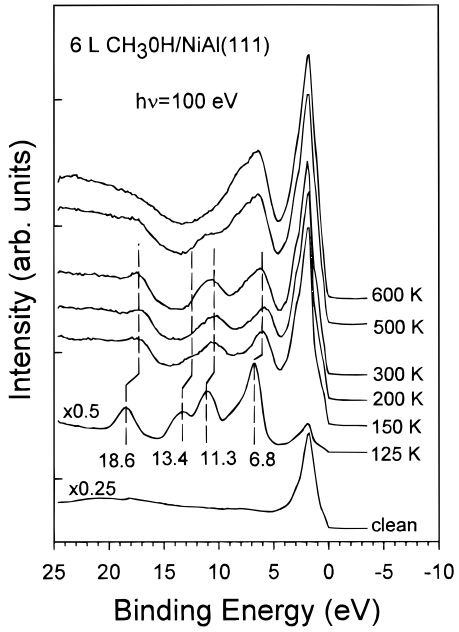

Figure 7. Valence band spectra of NiAl(111) after exposure to 6.0 langmuirs of CH_3OH at 120 K and after heating the surface to the indicated temperatures.

The low-exposure spectra obtained at 0.5 and 1 langmuir of CH_3OH all show the features present in the multilayer spectrum, suggesting that a significant portion of the impinging CH_3OH adsorbs molecularly at 130 K. It is noted that all the levels exhibit a shift to lower binding energy relative to the multilayer spectrum. We are not able to conclude whether this shift is due to an alteration of the methanol electronic states due to the surface bond or to differences in final state effects between the monolayer and multilayer. An exposure of 2 or 4 langmuirs results in a binding energy shift of the different levels back to where they reside after a 6 langmuir exposure and conclude from this that multilayer methanol begins to form after a ≥2 langmuir exposure.

Figure 7 exhibits valence band spectroscopy data that support the EELS identification of methoxy on NiAl(111) and adds some additional insight into the adsorption of CH_3OH on NiAl(111). These experimental data are obtained by exposing NiAl(111)

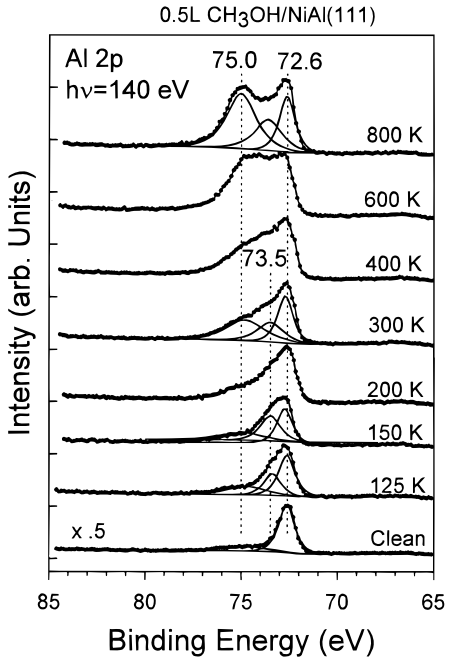

Figure 8. Al 2p data obtained after NiAl(111) has been exposed to 0.5 langmuir of CH_3OH at 120 K and after annealing to the indicated temperatures. The Al 2p of clean NiAl(111), Al−OCH_3, and Al_xO_y have been assigned to binding energies of 72.6, 73.5, and 75.0 eV. The fits only are to guide the eye, since it is emphasized that the Al $2p_{3/2}$ and $2p_{1/2}$ contributions (∼0.3 eV) have not been taken into account.

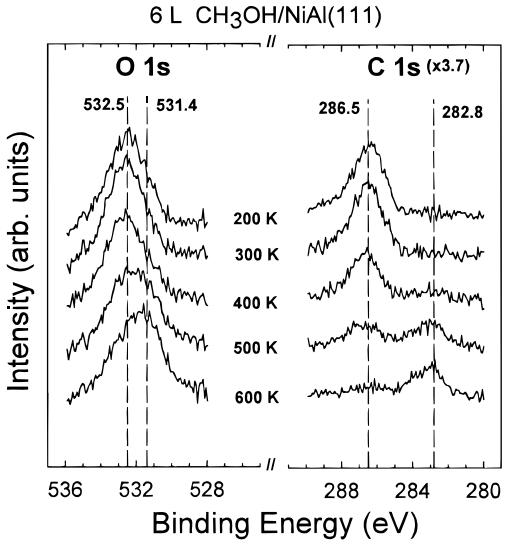

Figure 9. O 1s and C 1s XPS spectra obtained after NiAl(111) has been exposed to 6.0 langmuirs of CH_3OH at 120 K. All spectra are taken at 120 K after heating the surface to the indicated temperatures. Surface methoxy (at 200 K) is characterized by O and C 1s peaks at 532.5 and 286.5 eV, respectively.

to 6 langmuirs of CH_3OH at 125 K and then heating the surface in a stepwise fashion to the indicated temperatures. Heating the CH_3OH multilayer to 150 K results in a spectrum that is similar to either the 0.5 or 1 langmuir spectra of the preceding figure. We infer from this result that molecular methanol is present on the surface at 150 K and is coadsorbed with methoxy (shown to be present by EELS at 150 K). Heating to 200 K and then to 300 K progressively reduces spectral weight near 13 eV that has been attributed to the 5a′ level of methanol. We suspect that this is due to the completion of the O−H bond breaking step that must precede the formation of methoxy. In this temperature range we assign the 5.9, 10.7, and 17.8 eV features to the 2e, (1e + $5a_1$), and the $4a_1$ valence levels of methoxy, respectively (using C_{3v} classification).[42] This is consistent with the formation of methoxy species on other surfaces.[9,11,36] There is some broadening of the valence features in the 300 K spectrum, and we suspect that this may be due to some dissociation of the methoxy or alteration of the NiAl surface layer as was mentioned when discussing EELS data at this temperature. Further heating to 500 K decomposes the majority of methoxy (consistent with the TPD results), and by 600 K aluminum oxide is the only surface phase that can be discerned.

Figure 8 presents Al 2p core level spectra of NiAl(111) after exposure to 0.5 langmuir of CH_3OH at 120 K and subsequent stepwise annealing to higher temperatures. The Al 2p spectrum of clean NiAl(111) exhibits a binding energy of 72.6 eV. Adsorption of 0.5 langmuir of CH_3OH on the alloy surface at 125 K leads to a spectral broadening, relative to the clean spectrum, to the high binding energy side of the Al 2p feature. This broadening is presumably due to the interaction of CH_3OH and/or $CH_3O_{(ad)}$ with the Al component of the alloy. (Due to lack of sensitivity to Ni core levels with the photon energy used, analogous data for Ni were not obtained.) Heating the surface to 150 K leads to further broadening, and at this temperature a significant part of the Al 2p shift is due to the binding of methoxy (based on previously presented EELS data). It is estimated from the curve fitting shown in the figure that the Al 2p feature due to methoxy and/or methanol adsorption resides at ∼73.5 eV, 0.9 eV higher in binding energy than the Al 2p binding energy of clean NiAl(111). Both these spectra also contain a contribution from a relatively small amount of oxide contamination on the surface at 75 eV.[41] This contamination level is quite low and is below the detection limit of conventional XPS and AES. We emphasize that the fitting procedure is performed primarily to guide the eye to what we believe are the different spectral contributions. The $2p_{1/2}$ and $2p_{3/2}$ splitting of the Al 2p level has not been addressed (∼0.3 eV splitting) in this fitting procedure. Annealing the methoxy overlayer to 200 K results in a broadening to the high binding energy side of the Al 2p spectral region, and this broadening becomes more noticeable in the 300 K spectrum. Inspection of the spectral fitting of this latter spectrum suggests that the oxide feature has grown significantly, indicating that decomposition of the methoxy overlayer is occurring. EELS results presented above show that the vibrational mode intensity near ∼530 cm^{-1} grows upon heating from 200 to 300 K. It is surmised that this change in the EEL spectrum may be due to some oxidation of a fraction of the Al component of NiAl(111). Growth of spectral weight near 75 eV becomes more severe after heating to higher temperature. At an annealing temperature of 800 K (and also at 600 K), aluminum oxide is the dominant species. It is mentioned that the 800 K spectrum has Al 2p spectral weight in the same spectral region that we associated with the Al−methoxy interaction in the lower temperature data. EELS shows that methoxy is completely decomposed at a temperature of 800 K, and therefore the spectral weight between 73 and 75 eV in the high-temperature spectra is not due to methoxy, but instead is most likely due to the presence of nonstoichiometric Al oxides. Finally, annealing to 800 K causes the metallic Al spectral weight to increase relative to the lower temperature data. This increase in intensity of the metallic aluminum feature is believed to be due to surface segregation of aluminum, which has been observed previously in aluminide oxidation studies.[39]

3.4. X-ray Photoelectron Spectroscopy. Figure 9 exhibits O and C 1s XPS data for NiAl(111) that has been exposed to 6.0 langmuirs of CH_3OH at 120 K and subsequently annealed

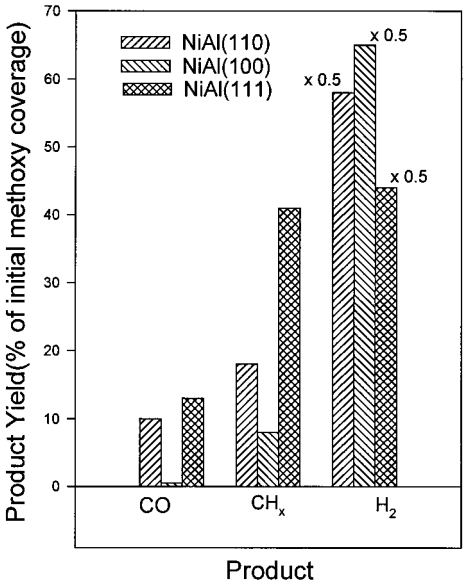

Figure 10. A comparison plot of the product yields (as a function of the percentage of the initial methoxy coverage) for CH_3OH/NiAl(110), CH_3OH/NiAl(100), and CH_3OH/NiAl(111). CH_x includes contributions from both CH_4 and CH_3. Note that CH_4 is only believed to be produced on NiAl(111) and NiAl(110). The (111) surface is the most reactive surface and produces largest amounts of CO and CH_x.

to the indicated temperatures. Spectra obtained after heating to 200 K exhibit O and C 1s peaks at 532.5 and 286.5 eV, respectively, that are assigned to methoxy. The thermal stability of methoxy has already been detailed with EELS and photoelectron spectroscopy. With regard to these XPS data, it is only mentioned that the decomposition of methoxy with increasing surface temperature results in a shift of the O 1s binding energy to 531.4 eV due to the formation of surface oxygen and a shift of the C 1s binding energy to 282.8 eV resulting from the formation of surface carbon. These binding energies for methoxy and the shifts due to the decomposition thereof are consistent with those obtained for methoxy on NiAl(110)[32a] and NiAl(100).[21]

These XPS data, unlike the EELS and synchrotron-based studies, however, allow us to estimate the relative yield of products by analyzing the decrease in spectral peak area for the O 1s and C 1s data as a function of annealing temperature in view of the TPD data presented earlier. For example, the decrease of the O 1s peak area between 300 and 500 K is used in the estimate of CO production as a percentage of the initial methoxy coverage at 150 K. Figure 10 plots these data and compares relative yield results for NiAl(111) to the CH_3OH/NiAl(110) and CH_3OH/NiAl(100) systems.[21] While these data will be discussed in a later section, it is mentioned that NiAl(111) is most active toward CO and CH_x production, where CH_x is used to denote the total yield of CH_4 and CH_3. Also, the reduced H_2 yield for NiAl(110) and NiAl(111) is due to the larger amount of the hydrogen that is incorporated into the CH_4 product.

4. Discussion

Results presented in the preceding section allow us to develop a picture of the thermal chemistry of CH_3OH on NiAl(111). On the basis of these results, the following general reaction scheme best summarizes the chemisorption and subsequent reaction steps (T_p is peak temperature):

$$CH_3OH_{(g)} \rightarrow CH_3OH_{(ad)} \quad \{120\ K\}$$

$$CH_3OH_{(ad)} \rightarrow CH_3O_{(ad)} + H_{(ad)} \quad \{150\ K\}$$

$$2H_{(ad)} \rightarrow H_{2(g)} \quad \{250-700\ K\}$$

$$CH_3O_{(ad)} + H_{(ad)} \rightarrow CH_{4(g)} + O_{(ad)} \quad \{T_p(CH_4) = 350\ K\}$$

$$CH_3O_{(ad)} \rightarrow CO_{(g)} + H_{2(g)} \quad \{T_p(CO) = 425\ K\}$$

$$CH_3O_{(ad)} \rightarrow CH_{3(g)} + O_{(ad)} \quad \{T_p(CH_3) = 550\ K\}$$

As summarized above, methanol decomposition on NiAl(111) produces a variety of gaseous products that include CH_4, CH_3, CO, and H_2. Decomposition of methanol on an sp metal such as aluminum[7-10] has been shown previously to result in the cleavage of the C−O bond to yield CH_4 and H_2, while on Ni,[12-17] the primary products are CO and H_2. In general, the gaseous product distribution experimentally observed for CH_3OH/NiAl(111) is what might of been expected from a simple combination of the product distribution of the individual monometallic components. The details of the chemistry that precedes the formation of these products, however, are unique to the alloy and do not appear to be describable in terms of pure Ni and Al chemistry. CO production, for example, is reaction rate limited on NiAl(111), while on Ni,[14,17] it is desorption limited. This statement for CH_3OH/NiAl(111) is based on EELS and valence band data that show that methoxy decomposes concurrently with CO production between 400 and 500 K. Also, the H_2 desorption temperature coincides with that for CO desorption, suggesting that the dehydrogenation of methoxy results in the simultaneous formation of gaseous CO and H_2. Furthermore, TPD of CO/NiAl(111) carried out in our laboratory shows that CO desorbs near 375 K, a lower temperature compared to its production via CH_3OH decomposition.

While CO is a significant fraction of the gaseous product that desorbs from NiAl(111), its production is associated with the decomposition of only ∼13% of the methoxy overlayer, originally present at 200 K. Perhaps, not surprisingly, the high affinity of Al for oxygen results in the majority of methoxy decomposing to surface oxygen. Inspection of Figure 10 shows that CH_3OH decomposition on NiAl(110) leads to a similar scenario where a similar amount of methoxy decomposition results in the formation of CO. In view of the experimental observation that there is no CO production from methoxy decomposition on Al-terminated NiAl(100), it is postulated that this product requires the presence of Ni in the outermost layer during the decomposition reactions of CH_3OH.

With regard to this point, concerning the effect of the different crystallographic planes, it is useful to compare EELS results for methoxy on all three surfaces. Table 1 exhibits vibrational modes for CH_3OH and CH_3O adsorbed on the low Miller indice planes of NiAl. For the present discussion the most revealing vibrational mode is the surface−OCH_3 stretch [i.e., ν(M−O)]. Methoxy on the Al-terminated (100) plane of NiAl exhibits a ν(M−O) mode at 640 cm^{-1},[21] close to the position of the same mode of methoxy adsorbed on monometallic Al (650 cm^{-1}).[7] The frequency of this mode is significantly lower (530 cm^{-1}) for methoxy adsorbed on the (110) plane[32a] that is capped by a well-ordered Ni and Al (50% each component) surface layer. As mentioned in the Introduction, the structure of the (111) plane is more complex, since it is thought to be comprised of 1×1 domains that are individually terminated by Al and Ni. EELS results presented in this study suggest that methoxy exhibits two ν(M−O) modes at ∼530 and 630 cm^{-1}. We feel this

experimental observation is noteworthy, since it suggests that methoxy probably resides on at least two types of surface binding sites. Whether these sites correspond to the two proposed domains of NiAl(111) is not known, but it does suggest that one species resides on a site that is strongly influenced by Ni whereas another appears to have predominately Al character. [The presence of more than one methoxy species also would seem to be consistent with our experimental observation that the widths of the EELS modes of methoxy are greater when adsorbed on NiAl(111) than on NiAl(110) or NiAl(100).]

Production of CO on NiAl(111) indicates that a certain fraction of adsorbed methoxy is weakly enough bound so that the surface−oxygen bond can be broken. This presumption is qualitatively consistent with methoxy exhibiting the lower stretching frequency 530 cm^{-1} mode on the planes that contain Ni in the outermost layer and that produce CO. It is mentioned, however, that CH_4 is also a significant gaseous product on NiAl(111) and NiAl(110), emphasizing that these sites still have strong Al character. We suspect that the ∼640 cm^{-1} mode is associated with methoxy bound on more "Al-rich" sites of NiAl(111) based on our EELS results for methoxy on the (100) plane. These "Al-rich" sites may be on those domains that are Al terminated. In any case these sites appear to bind the methoxy most strongly and inhibit the formation of any oxygenated gaseous product.

While these proposed assignments and interpretation are, for the most part, consistent with our experimental observations, there is some ambiguity. Methoxy adsorbed on NiAl(110) exhibits a single surface−OCH_3 mode (within our experimental resolution) at 530 cm^{-1}, but this surface exhibits a significant amount of chemistry that is similar to the Al-terminated (100) plane, such as oxide formation and methyl ejection (attributed to the strong Al−O bond). It is suspected that the presence of methoxy at low temperature (≤200 K) occurs without a gross distortion of the surface atomic composition and structure. As the methoxy starts to compose at higher temperature, it is expected that there is a significant amount of surface reconstruction as Ni−Al bonding is disrupted due to the formation of strong Al−O bonds and eventually the oxide thereof. CO production at 425 K and methane formation near 350 K probably occur at a low enough temperature where the Ni −Al interaction is significant in the outermost layer and exerts a significant influence on the reaction mechanism. The evolution of CH_4 at this low temperature is consistent with a strong Al−OCH_3 interaction but also implies a strong Ni contribution, since the hydrogenation of hydrocarbon fragments to CH_4 occurs on Ni in a vacuum.[43,44]

Methyl radicals desorb from NiAl(111) with a peak temperature of 580 K. Prior research shows that methyl desorbs from NiAl(100)[21] and NiAl(110)[32a] at a similar temperature, suggesting that this reaction step is dominated by the Al component of the alloy and probably does not require the transition metal to directly bind to the adsorbate. At a temperature of 580 K there undoubtedly is surface oxygen and carbon that probably suppresses dehydrogenation of methoxy so that methyl desorption can occur. This type of process has been experimentally observed to occur during the decomposition of methoxy on O/Mo(110)[44] and has also been addressed by calculation.[45,46] While the methoxy that decomposes to form methyl radical is probably bound directly and exclusively to Al, the transition metal does have an effect on this decomposition process. Recent research in our laboratory has shown that the thermal decomposition of methoxy to produce methyl radical is sensitive to the nature of the transition metal component of the transition metal−aluminum alloy. For example, methyl desorption occurs near 580 K on CH_3OH/NiAl(111) and CH_3OH/NiAl(100), but this same process occurs on Al-terminated FeAl(100) and TiAl(010) at 550 and 450 K, respectively,[47] showing the influence of the transition metal component.

5. Summary

Photoelectron spectroscopy and EELS suggest that methanol adsorbs molecularly on NiAl(111) at 120 K. Based on these same techniques, thermal annealing to 150 K results in the formation of $CH_3O_{(ad)}$. Further heating to 200 K completes the scission of the O−H bond and forms a methoxy overlayer. The resulting intermediate species begins to decompose at temperatures between 200 and 300 K. A variety of gaseous products, which include CH_4, CH_3, CO, and H_2, desorb during the decomposition of methoxy between 300 and 650 K. EELS results suggest that methoxy may adopt two different binding sites on NiAl(111): one with a strong contribution from Ni and another that has a lesser Ni influence and is richer in Al character. Methoxy decomposition on the former type of site may be responsible for CO and CH_4 production, since the presence of Ni in the outermost layer appears to be a prerequisite for the production of these products.

Acknowledgment. Support of this research by the National Science Foundation (DMR #9258544) is gratefully appreciated. Research was carried out in part at the National Synchrotron Light Source, Brookhaven National Laboratory, which is supported by the U.S. Department of Energy, Division of Materials Sciences and Division of Chemical Sciences.

References and Notes

(1) Nieuwenhuys, B. E. In *The Chemical Physics of Solid Surfaces;* King, D. A., Woodruff, D. P., Eds.; Elsevier: Amsterdam, 1993; Vol. 6, p 185.
(2) Kester, K. B.; Falconer, J. L. *J. Catal.* **1984,** *89*, 380.
(3) Kester, K. B.; Zagh, E.; Falconer, J. L. *Appl. Catal.* **1986,** *22*, 311.
(4) Mirodatos, C.; Praliaud, H.; Primet, M. *J. Catal.* **1987**, *107*, 275.
(5) Glugla, P. G.; Bailey, K. M.; Falconer, J. L. *J. Phys. Chem.* **1988,** *92*, 4474.
(6) Wise, H.; Oudar, J. *Material Concepts in Surface Reactivity and Catalysis;* Academic Press: San Diego, 1990; p 113.
(7) Basu, P.; Chen, J. G.; Ng, L. I.; Colaianni, M. L.; Yates, Jr., J. T. *J. Chem. Phys.* **1988**, *89*, 2406.
(8) Chen, J. G.; Basu, P.; Ng., L.; Yates, Jr., J. T. *Surf. Sci.* **1988,** *194*, 397.
(9) Rogers, J. W.; Hance, Jr., R. L.; White, J. M. *Surf. Sci.* **1980,** *100*, 388.
(10) Tindall, I. F.; Vickerman, J. C. *Surf. Sci.* **1985,** *149*, 577.
(11) Rubloff, G. W.; Demuth, J. E. *J. Vac. Sci. Technol. A* **1977,** *14*, 419.
(12) Vajo, J.; Campbell, J. H.; Becker, C. H. *J. Phys. Chem.* **1991,** *95*, 9457.
(13) Vajo, J.; Campbell, J. H.; Becker, C. H. *J. Vac. Sci. Technol. A* **1989,** *7*, 1949.
(14) Richter, L. J.; Ho, W. *J. Chem. Phys.* **1985,** *83*, 2569.
(15) Richter, L. J.; Ho, W. *J. Vac. Sci. Technol. A.* **1985,** *3*, 1549.
(16) Richter, L. J.; Gurney, B. A.; Villarrubias, J. S.; Ho, W. *Chem. Phys. Lett.* **1984,** *113*, 185.
(17) Bare, S. R.; Stroscio, J. A.; Ho, W. *Surf. Sci.* **1985,** *150*, 399.
(18) Johnson, S.; Madix, R. J. *Surf. Sci.* **1981,** *103*, 361.
(19) Gates, S. M.; Russell, J. N.; Yates, Jr., J. T. *J. Catal.* **1985,** *92*, 25.
(20) Gates, S. M.; Russell, J. N.; Yates, Jr., J. T. *Surf. Sci.* **1985,** *159*, 233.
(21) Sheu, B. R.; Strongin, D. R. *J. Catal.* **1995,** *154*, 379.
(22) Ross, P. N. *J. Vac. Sci. Technol. A.* **1992**, *10*, 2546.
(23) Yalisove, S. M.; Graham, W. R. *Surf. Sci.* **1987,** *183***,** 556.
(24) Davis, H. L.; Noonan, J. R. In *Physical and Chemical Properties of Thin Metal Overlayers and alloy Surfaces;* Zehner, D. M., Goodman, D. W., Eds.; Materials Research Society: Pittsburgh, PA, 1987; Vol. 83, p 3.
(25) Noonan, J. R.; Davis, H. L. *Phys. Rev. Lett.* **1987,** *59* (15), 1714.

(26) Noonan, J. R.; Davis, H. L. *J. Vac. Sci. Technol. A* **1988,** *6* (3), 722.

(27) (a) Chaturvedi, S.; Strongin, D. R. *Langmuir*. **1997**, *13*, 3162. (b) Chaturvedi, S.; Strongin, D. R. Manuscript in preparation.

(28) Gates, S. M.; Russell, J. N.; Yates, Jr., J. T. *Surf. Sci.* **1984,** *146*, 199.

(29) Hall, R. B.; Desantolo, A. M.; Bare, S. J. *Surf. Sci.* **1985,** *161*, L533.

(30) Hall, R. B.; De Santolo, A. M.; Grubb, S. G. *J. Vac. Sci. Technol. A* **1987,** *5*, 865.

(31) Chen, B.; Falconer, J. L. *J. Catal.* **1993**, *144*, 214.

(32) (a) Sheu, B. R.; Chaturvedi, S.; Strongin, D. R. *J. Phys. Chem.* **1994**, *98*, 10258. (b) Gleason, N. R.; Chaturvedi, S.; Strongin, D. R. *Surf. Sci*. **1995**, *326*, 27.

(33) Donnelly, V. M.; McCaulley, J. A. *Surf. Sci.* **1990**, *235*, L333.

(34) Osberghaus, O.; Taubert, R. *J. Phys. Chem.* **1955**, *4*, 264.

(35) Creighton, J. R. *Surf. Sci.* **1990**, *234*, 287.

(36) Witko, M.; Hermann, K.; Ricken, D.; Stenzel, W.; Conrad, H.; Bradshaw, A. M. *J. Chem. Phys.* **1993**, *177*, 363.

(37) Halverson, D. E.; Cocke, D. L. *J. Vac. Sci. Technol. A.* **1989,** *7*, 40.

(38) Thomas, S.; Sherwood, P. M. *Anal. Chem.* **1992,** *64*, 2488.

(39) Gleason, N. R. Ph.D. Thesis, SUNY at Stony Brook, 1995.

(40) Crowell, J. E.; Chen, J. G.; Hercules, D. M.; Yates, J. T., Jr. *J. Chem. Phys.* **1987**, *86*, 5804.

(41) Jaeger, R. M.; Kuhlenbeck, H.; Freund, H. J.; Wuttig, M.; lbach, H. *Surf. Sci.* **1991**, *259*, 235.

(42) Robin, M. B.; Kuebler, N. A. *J. Electron Spectrosc. Relat. Phenom.* **1972/1973,** *1*, 13.

(43) Tjandra, S.; Zaera, F. *Langmuir* **1992,** *8*, 2090.

(44) Tjandra, S.; Zaera, F. *J. Catal.* **1993,** *144*, 361.

(45) Serafin, J. G.; Friend, C. M. *J. Am. Chem. Soc*. **1989**, *111*, 8967.

(46) Shiller, P.; Anderson, A. B. *J. Phys. Chem.* **1991**, *95*, 1396.

(47) Anderson, A. B.; Jen, S. F. *J. Phys. Chem.* **1991,** *95*, 7792.

(48) Chaturvedi, S.; Strongin, D. R. *Catal. Lett.* **1997**, *47*, 105.